PAOLO BATTAINI
8853 S.p.a.
Pero (MI).

Paolo Battaini holds a degree in Nuclear Ingeneering, with a particolar focus on Materials. He has been designing and manufacturing alloys made of precious metals for dental and jewelry applications for more than 20 years. At present, he is consultant for 8853 SpA, where he is Responsible for Research and Development as well as for the manufacturing of semi-finished products for the jewelry industry. He is SME in the use of techniques regarding electronic scanning microscopy and he owns Esemir Sas, by means of which he is able to focus on failure analysis for different industrial fields. Moreover, he is lecturer on 'Processing Techniques' for the degree course on "Jewelry Science and Technology" at Bicocca University (Milan, Italy).

That the microstructure of a material is important is a well-known fact. The cause, and possible solution, of a problem that arises while working a precious alloy can be identified by studying the microstructure of the material. An optical stereo microscope is extremely useful in providing a three-dimensional (3D) view of a sample, but enlargement is limited. Furthermore, the most common techniques of micro-structural observation, such as optical metallography and scanning electron microscopy, usually only give a two-dimensional picture. Some techniques that provide a 3D view of the microstructure of a surface are now available but have yet to be widely adopted, especially in the gold sector. The aim of this paper is to show 3D images of the microstructure of some precious materials, like ruptured surfaces, different surface finishings or surface defects, and to highlight any additional information that 3D imaging can offer. Anaglyph images obtained using an scanning electron microscope will be used and the audience will be provided with special two-colour glasses.

Precious Metals Microstructures in 3D

The scanning electron microscope (SEM) is widely used in many industrial fields, as it offers images whose manifold characteristics are unique if compared with the information obtained by means of other more traditional techniques. Some among many are the high resolution, the wide range of magnification and the exceptionally high depth of field, i.e. the possibility of obtaining perfectly focused images of details placed at different levels.
Even though the SEM images look tri-dimensional, they are in fact bi-dimensional as the grey level of the pixels is not a function of the distance of the observed point, but depends on the material, the microstructural features of the surface and other material properties. Furthermore, the high depth of field sometimes makes it difficult to perceive the real distance between two objects, just because they are so well focused. For this reason efforts have been made to recover the third dimension of the SEM images. One of the techniques applied for this purpose is photogrammetry, which makes use of couples of stereo images to reconstruct the tri-dimensional view of a specimen.

Techniques of tri-dimensional characterization of surfaces at a microscopic level are required in many applications, both for qualitative and quantitative reasons[1].

The present work is aimed at describing in a simple way the so-called 'sample tilting' method, which allows for a tri-dimensional view of SEM images with the aid of special two-color glasses. The examples given in the following will concern goldsmith's materials and cast new light on well known concepts, not always understood in all their aspects though.

Principles of the stereo technique.

The human brain can get information about the distance of the observed objects by using the images acquired by both eyes. Our eyes are 6 to 10 cm far from each other and provide two slightly different views as shown in figure 1. This phenomenon, known as parallax, changes with the distance between the observer and what is observed. In fact the closer to the observer are the objects, the higher is the parallax. Our brain elaborates the parallax information and converts it into information about depth.
There are several methods to obtain images of the same object observed under two different orientations, so as to simulate what our eyes do. The two images are called 'stereo couple.' By hypothesizing that one of the two images is obtained with the left eye and the other with the right eye, it is possible to produce a 3D image with depth perception by properly combining the images of the stereo couple.

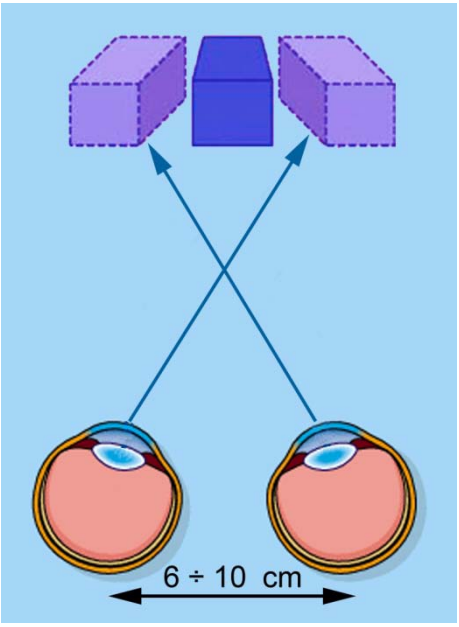

Figure 1.

The right eye sees the object as represented in the upper part of the drawing, on the left. The left eye does the opposite. The combination of the two images provides for the perception of the true depth, which is in the central part of the drawing.

One of the most popular techniques aimed at combining the two images consists in obtaining one in a false red color and the other in false blue or cyan. The two pictures are then overlapped by a proper image analysis software and the

resulting image is observed with special goggles provided with a red filter for the left eye and a blue or cyan one for the right one.
The combination of these two images in our brain occurs by means of the so-called 'retinal rivalry' defined as 'the oscillating perception of first one then the other of two visual stimuli which differ radically in color or form when they are presented simultaneously to congruent areas of both eyes'.

Figure 2.
Giovanni Battista della Porta (1535-1615).

This phenomenon was discovered and clearly described by the Italian humanist and scientist Giovanni Battista Della Porta [(2)] in 1593, as reported by Wade in his book "A natural history of vision" [(3)].
In SEM stereomicroscopy the most common method for obtaining the stereo couple is the so-called 'sample tilting', based on acquiring two images of the same point of a specimen, the second one after tilting properly. Figure 3 shows the SEM specimen chamber, particularly the specimen holder assembly. This arrangement allows for the shifting of the specimen along the three directions X, Y and Z, as well as the tilting around the direction Y.
This procedure is equivalent to observing the specimen under two different points of view. The tilt angle is normally around 6°, which is typical of the human eyes. Actually, the tilt to be used depends on many factors, such as magnification, surface roughness and the distance between the specimen and the final lens of the microscope, the so-called working distance. As a general rule, small tilt angles are needed at low magnification, whereas high angles are needed with not very rough surfaces.

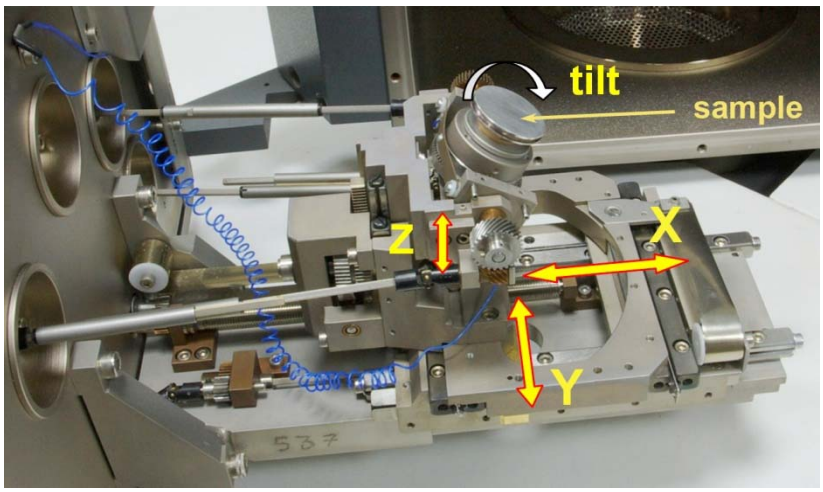

Figure 3.

The specimen stage of the scanning electron microscope enables the operator to move the specimen holder along the three directions X, Y and Z, and to tilt it around the Y axis.

When the specimen is tilted, it normally undergoes a lateral displacement so as to make it difficult for the operator to find the same area at the centre of the image. As a consequence, a low magnification image of the whole area must be obtained first, in order to find again the details for further analysis at high magnification and after tilting the specimen. Furthermore, as the tilt usually changes the height of the specimen, the resulting image may be out of focus, requiring the operator to readjust the specimen height to re-focus the image. The focusing system of the microscope is not to be used in this case, as it will cause a change of magnification.

In addition to the possibility of observing a specimen tri-dimensionally, the SEM technique provides also for quantitative measurements of its tri-dimensional characteristics.
When a surface is scanned , the electron beam is supposed to be focused on the surface along the Y axis and parallel to the optical axis (perpendicular to the focal plane), as shown in figure 4. In the so-called eucentric position, the tilt does not cause any displacement along the Y axis. Point B is above point A by an unknown distance BC before tilting the specimen. The projection of the segment AB on the focal plane is segment AC. After tilting the specimen by an angle the two distances will become AB' and AC'. Point B will move to point B'. This displacement is also known as 'parallax displacement'.

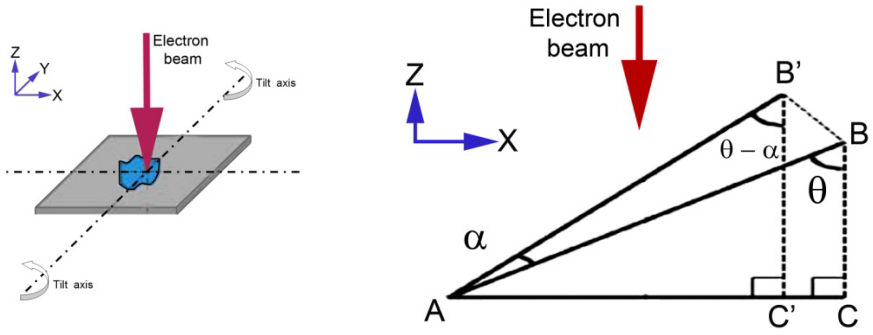

Figure 4.
On the left: the scheme of observation of a specimen in the SEM specimen chamber. The specimen is tilted around the Y axis. On the right: the displacement of point B with respect to point A, after tilting the specimen by an angle .

With reference to figure 4, the following geometric correlation exists

$$\frac{AC}{\sin\vartheta} = \frac{AC'}{\sin(\vartheta - \alpha)} \qquad \frac{AC}{BC} = \tan\theta$$

where AC and AC' can be measured on the SEM stereo couple images, whereas the angle is known.
According to the formulas above and remembering that $\sin(\vartheta - \alpha)$ = sin ϑ cos cos ϑ sin , the height BC can be calculated as

$$BC = \frac{\left(AC\cos\alpha - AC'\right)}{\sin\alpha} \cong \frac{P}{\sin\alpha}$$

where P is the displacement from B to A, which is the parallax value. The approximation applies to small values of like those considered here, that is when cos is approximately equal to 1.

Examples

Some examples of microstructures analyzed by SEM are reported in the following. Their interpretation by means of tri-dimensional observation is more immediate and clearer, if compared with the usual bi-dimensional technique. The examples can be seen tri-dimensionally by using goggles provided with a red filter for the left eye and a cyan one for the right one.

Fractography.

The aim of fractography is to analyze the morphological aspects of a fracture and to find a relationship between the topography of the fracture surface and the causes and mechanisms which have produced it[4].

The first who used the description of a fracture surface to assess the quality of a metallurgical process was an Italian metallurgist, Vannoccio Biringuccio, in 1540. He used the morphology of a fracture as a means of quality assurance both for ferrous and non-ferrous alloys [5].

The rupture of metal alloys occurs in different ways which are to be understood in order to avoid inconveniences while processing manufactured products or using them. It can also be said that by causing the rupture of a specific alloy and observing how it develops it is possible to gain a lot of information about the physical and mechanical properties of the alloy[6].

One of the most significant sources of information about the causes of ruptures is the fracture surface itself, as it is the exact recording of the history of the rupture. The main technique suited to this kind of study is fractography carried out by scanning electron microscopy.

The tri-dimensional observation of the fracture surface provides most information about its morphology.
Four main rupture types exist, that is dimple rupture, cleavage, fatigue and de-cohesive rupture. As regards precious metals, dimple rupture is the most common. However, also the other ones may occur and if that happens it means there could be mistakes in the production process or even in the jewel designing.

The first example concerns the fracture surface of a specimen for tensile tests, made of an alloy of Pd950. The specimen has been obtained by investment casting. The rupture has been caused on purpose, in order to measure the mechanical properties of the alloy. The observation by SEM reveals two regions (figure 5), the first having a multifaceted microstructure and covering a little more than one third of the section, the second characterized by a more irregular microstructure and appearing on the left, elongated towards the observer.

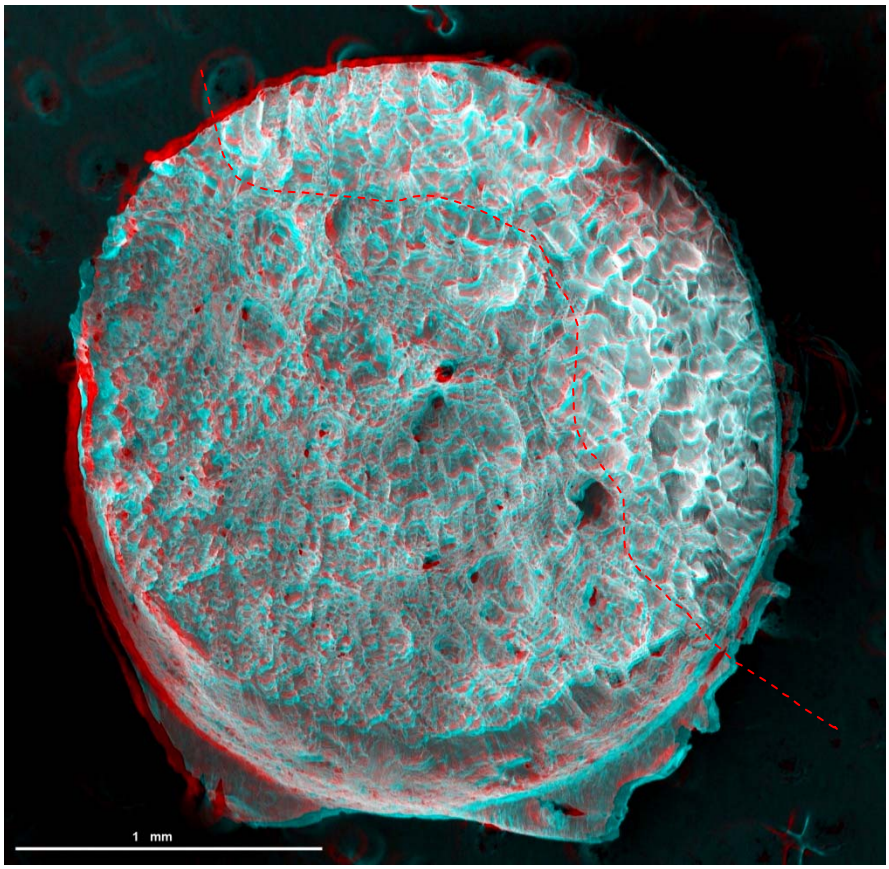

Figure 5.

Fracture surface of a specimen made of a Pd 950 alloy. Two morphologically different regions appear on the surface, as shown by the dashed line. The portion on the right has a multifaceted aspect, whereas the one on the left is more irregular.

At higher magnification (figure 6) the left part of the fracture surface reveals the presence of dimples, typical of ductile materials, which show high plastic and permanent deformation prior to rupture.

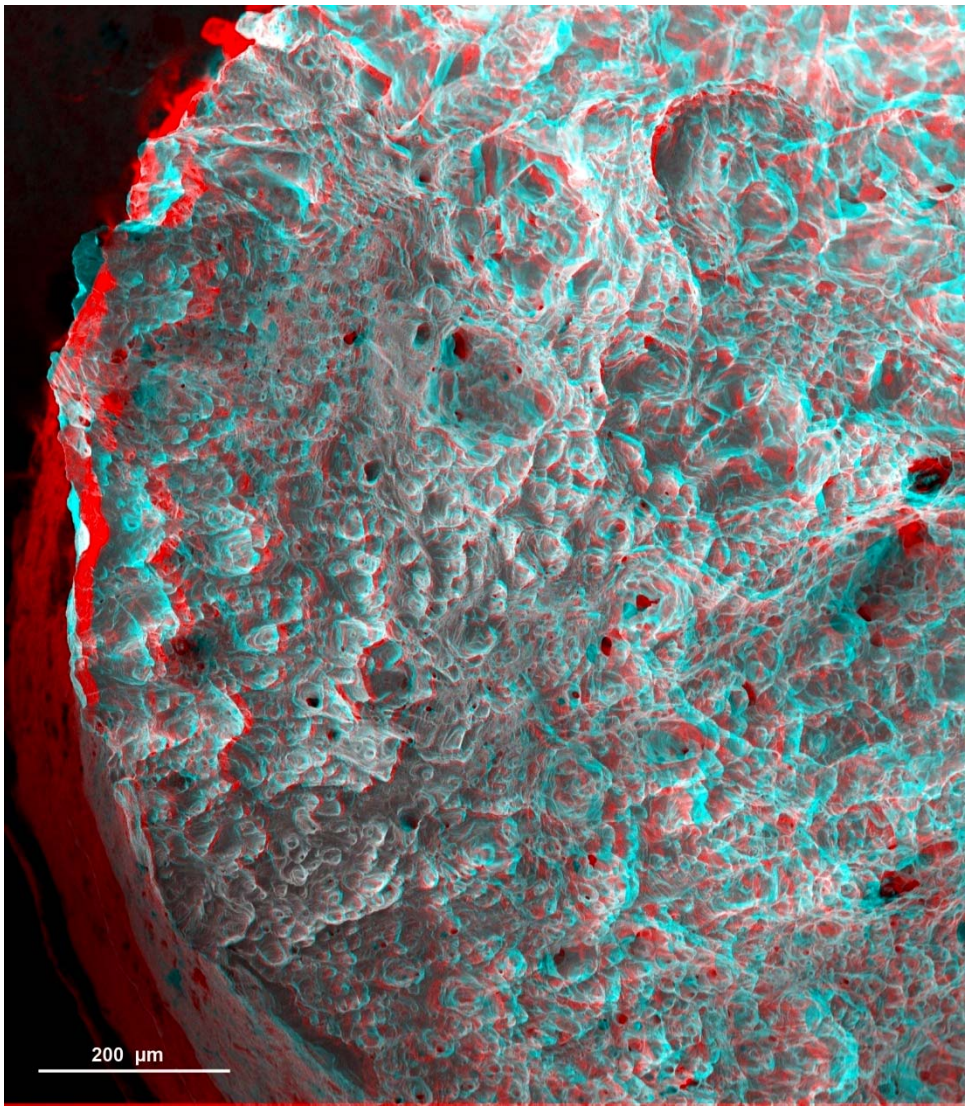

Figure 6.

This part of the fracture surface represents very clearly the high ductility properties of the material. In fact, not only is the left part elongated upwards - as it is the final tear zone, but also the typical dimples are visible on the whole surface. See more details in figure 7.

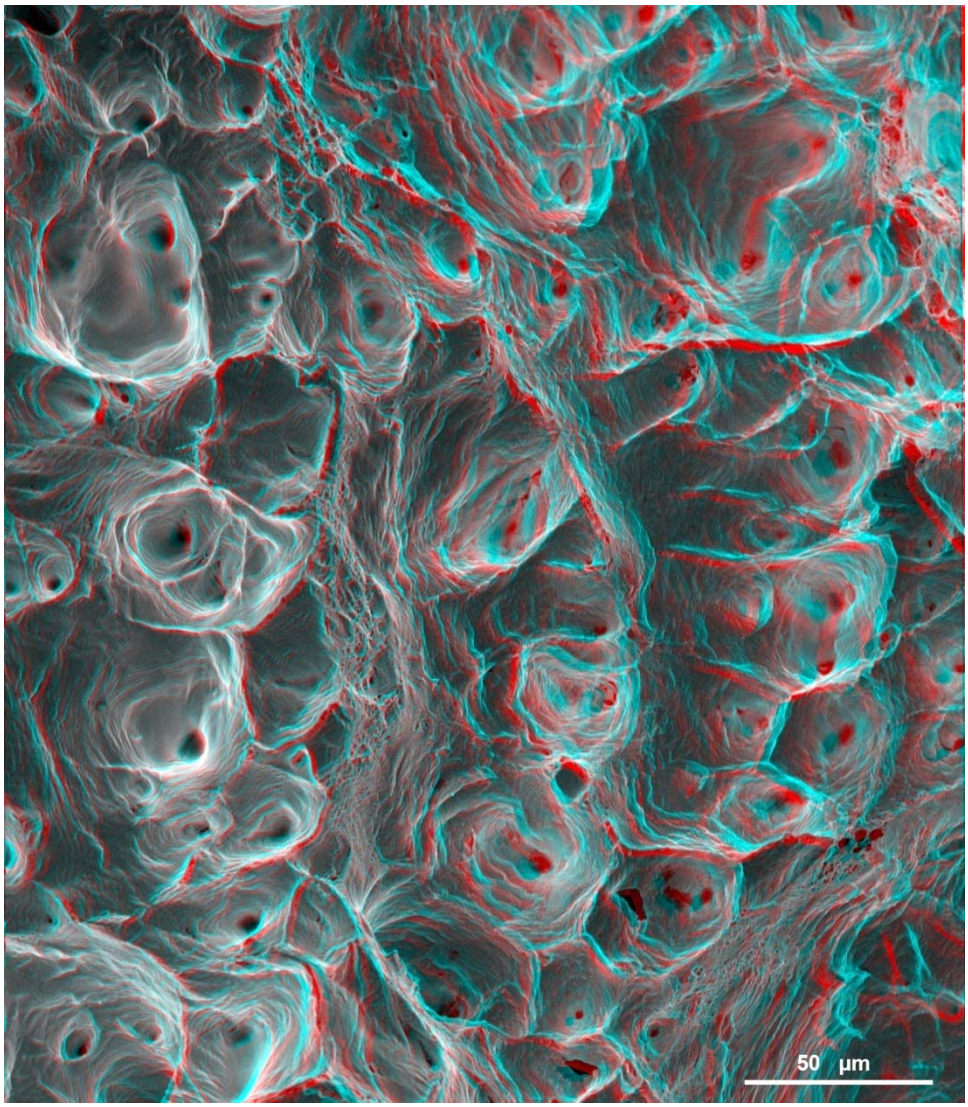

Figure 7.

Detail of the central part of figure 6, showing the dimples, typical of a ductile rupture. The dimples appear as cones produced by plastic deformation, whose central region shows spherical cavities. Such cavities are probably due to gas porosity, which have initiated the rupture process. The information provided is that this microstructural defect was present in the alloy before the rupture.

By observing at even higher magnification, it is possible to detect a distribution of small gas porosity at the center of the dimples. The dimples appear as upside down cones, whose vertexes are the pores which have initiated them. The material has deformed around the pores, giving rise to the dimples.
By further zooming (figure 8), even smaller dimples can be detected, initiated by other smaller-scale defects.

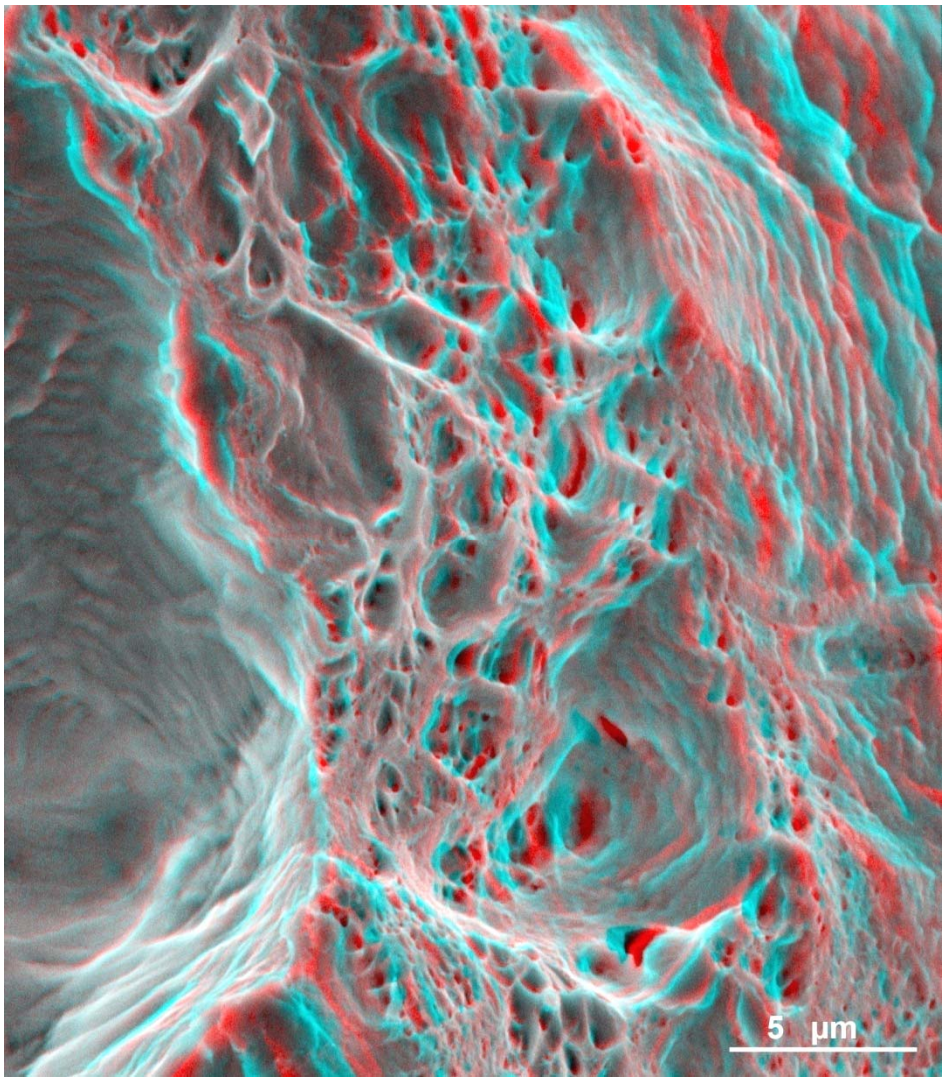

Figure 8.

Detail of figure 7 showing other dimples. In this case the defects responsible for rupture initiation are smaller and part of them still consists of gas porosity.

The right part of the fracture surface (figure 5) discloses another major property of this alloy. In this region the rupture is due to de-cohesion at the grain boundaries (figure 9). What is to be understood is why the alloy has ruptured in two different ways.

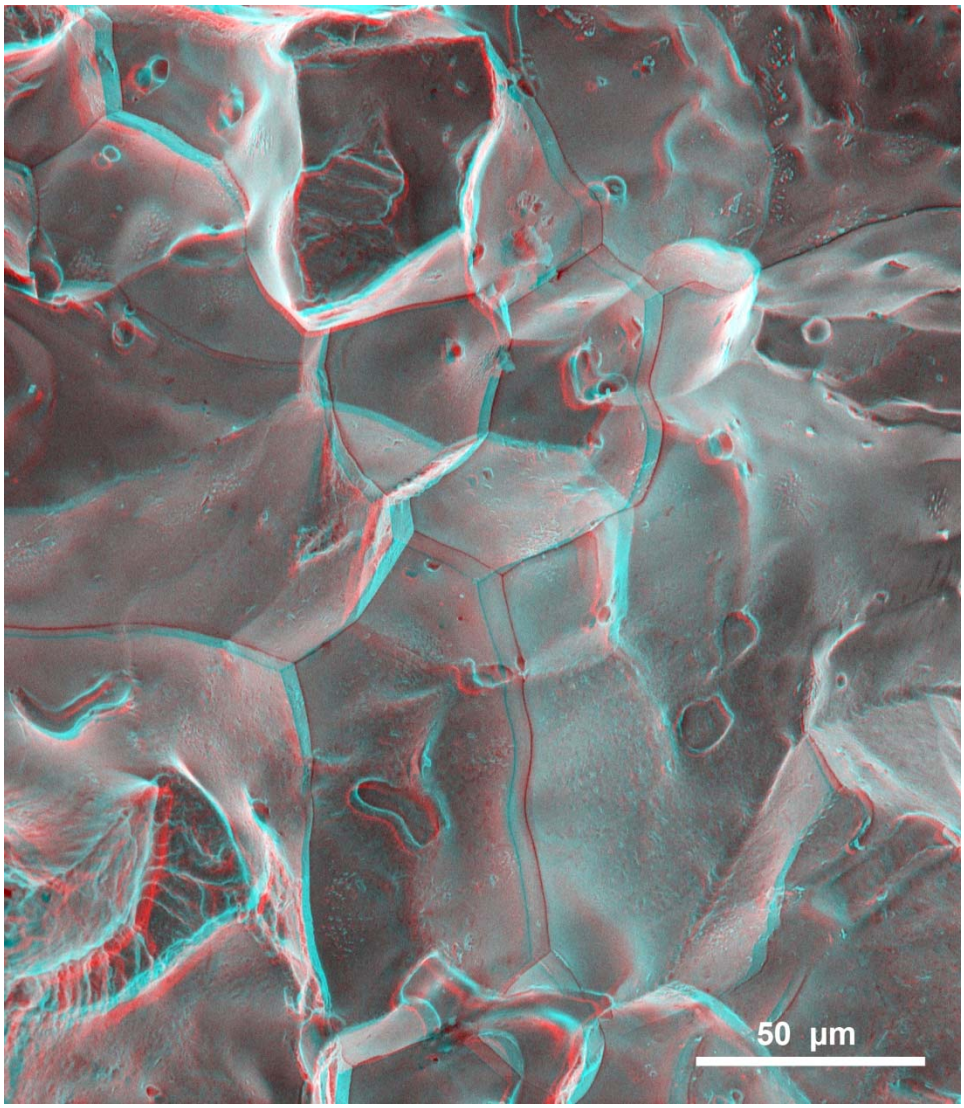

Figure 9.

The right region of the fracture surface (figure 5) shows a completely different situation. Rupture has occurred by de-cohesion along the grain boundaries (intergranular rupture).

The answer to this question lies in the wavy decorations which appear as protuberances on some grain boundaries (figure 10).
These are due to hot tearing, i.e. when the grain boundaries detach at high temperature, or during cooling in the flask, or even before, during solidification of the alloy. The fractographic analysis performed on this specimen proves that the investigated alloy has undergone hot tearing. As a consequence, despite being ductile at room temperature, the alloy goes through grain boundary brittleness during and soon after solidifying[7].

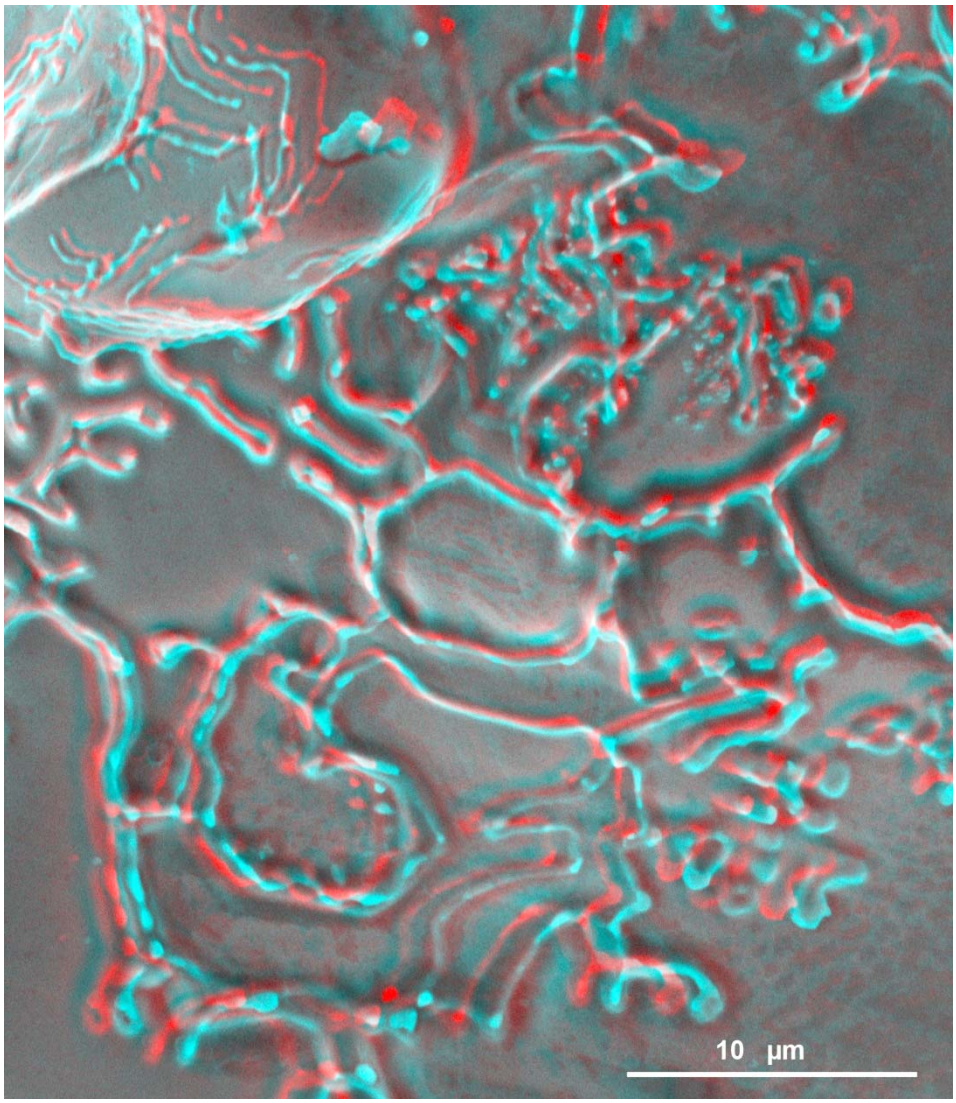

Figure 10.

Wavy intergranular decorations accompanying grain decohesion at high temperature are revealed. This phenomenon is also known as hot tearing.

The tri-dimensional observation of figures 9 and 10 reveals the shape of crystal grains in space and the protuberance of the wavy decorations where the final detachment has occurred.

The second example concerns another Pd 950 alloy. Unlike the previous case, this alloy is not in the as cast condition, but is given as a drawn wire, annealed several times. The wire has also undergone a tensile test until rupture. The SEM observation of its fracture surface shows that the material deforms plastically to a much larger extent than in the previous case prior to final rupture (figure 11).

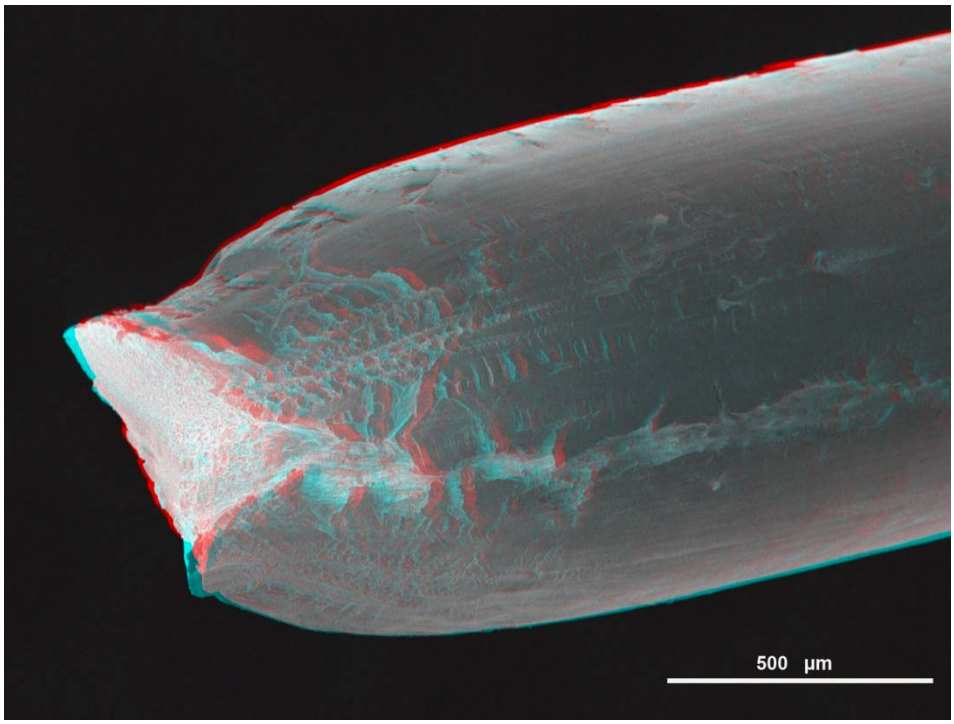

Figure 11.

The Pd 950 wire ruptured after tensile test shows a much higher plastic deformation than the investment casting specimen.

The typical cup-and-cone shape of the rupture zone, clearly visible in 3D mode (figure 11 and 12) shows that the first part to collapse is the one along the wire axis, at the center of the fracture surface, with a fiber-like morphology (figure 13). Then the rupture ends on the outer shear-lip zone (figures 14 and 15).

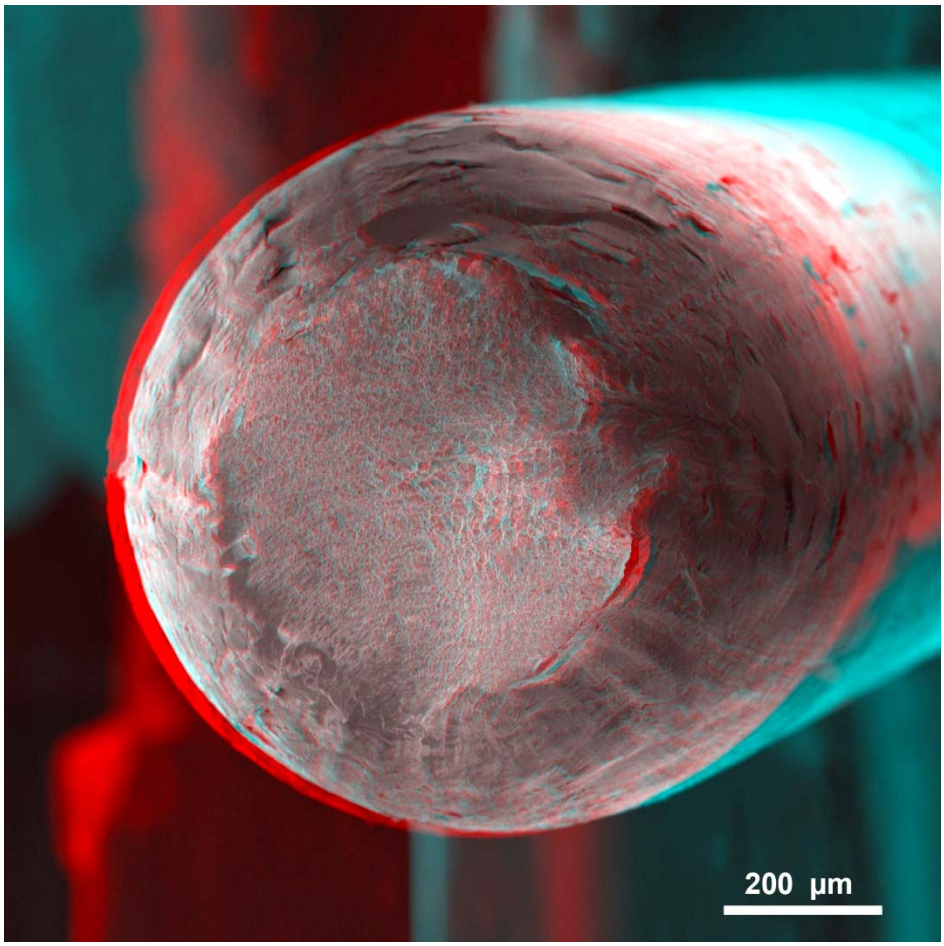

Figure 12.

Fracture surface of the Pd950 alloy wire. The fracture surface, observed in three-dimension, shows the characteristic cup-and-cone aspect, typical of ductile materials.

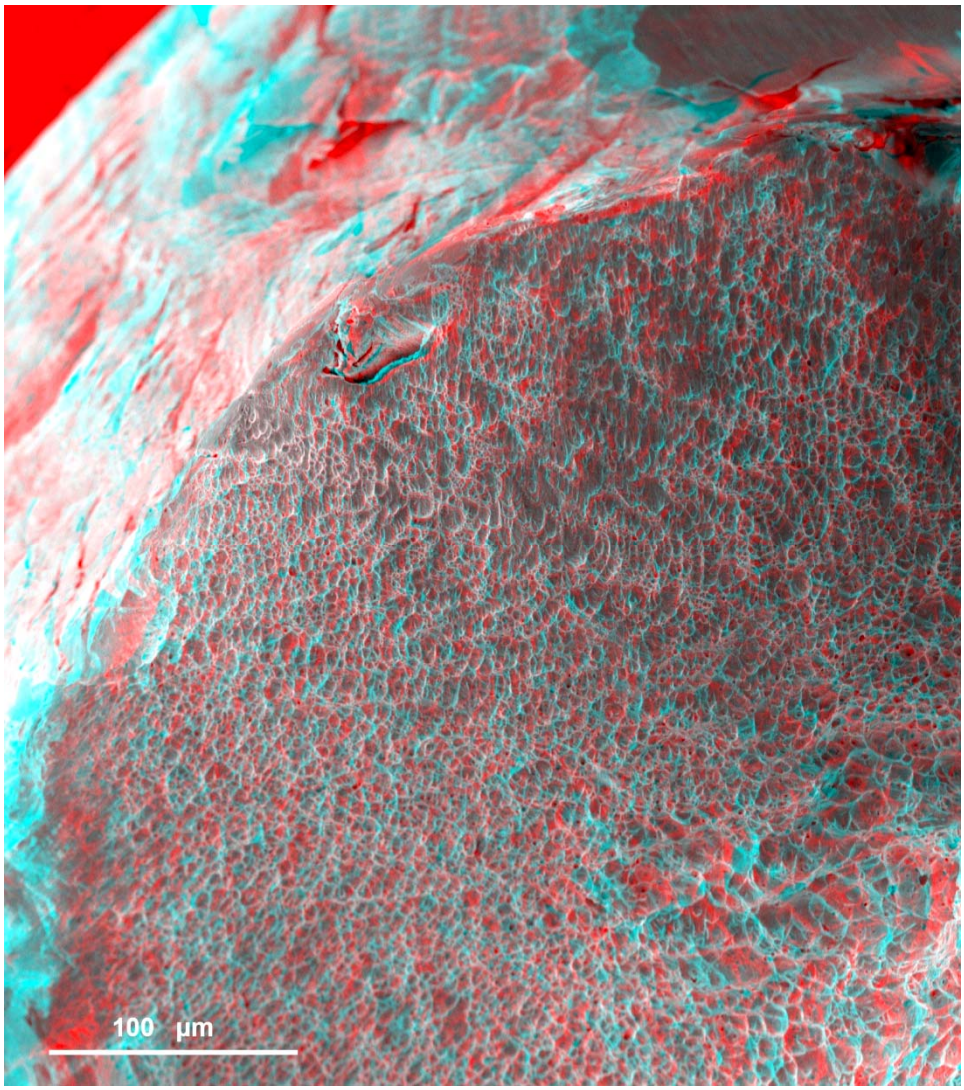

Figure 13.

Detail of the fracture surface. The surface is covered with dimples, whose size increases as approaching the center of the specimen.

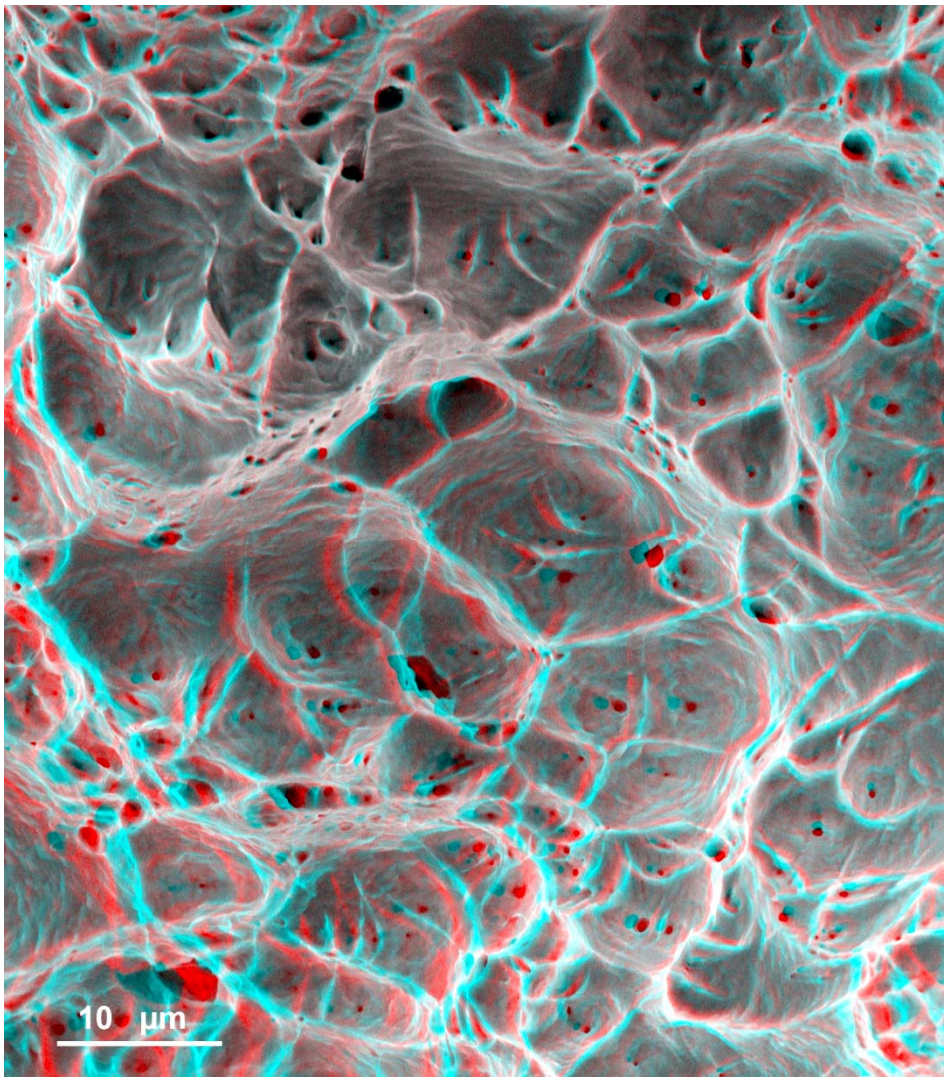

Figure 14.

Central part of the fracture surface. Here the dimples are cup-shaped with upward lips. This means that the rupture has occurred by axial tearing. The dimples opened around voids or defects whose size is larger in the central region of the Pd950 wire.

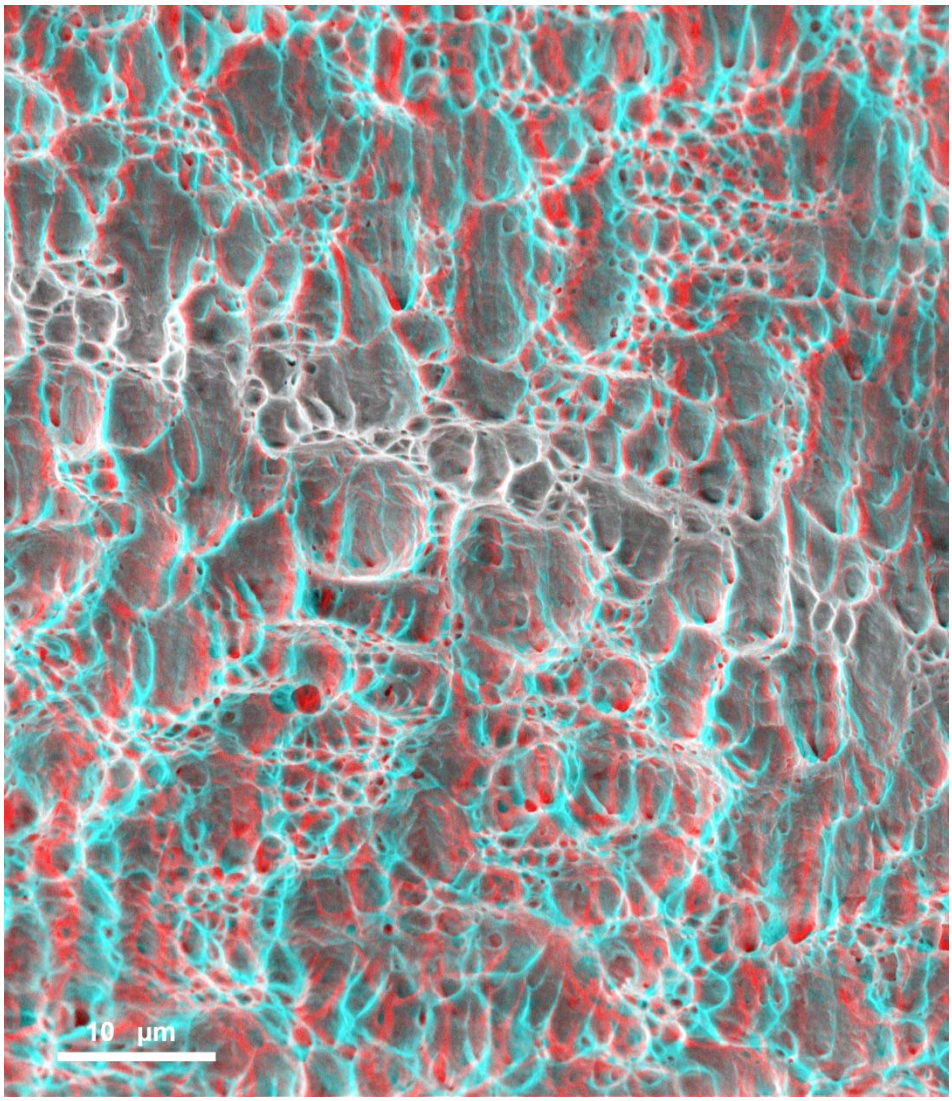

Figure 15.

Detail of the outer region of the fracture surface of figure 13, photographed at the same magnification as in figure 14.
The cup-shaped dimples are clearly visible by tri-dimensional observation.
The shape of the dimples proves that the fracture propagated from the bottom to the top part of the photographed region, that is from the center to the surface of the wire.

The last example concerns the fire cracked surface of an 18-carat nickel white gold tube[8]. The longitudinal fracture surface appears rather flat, even if observed tri-dimensionally (figure 16).

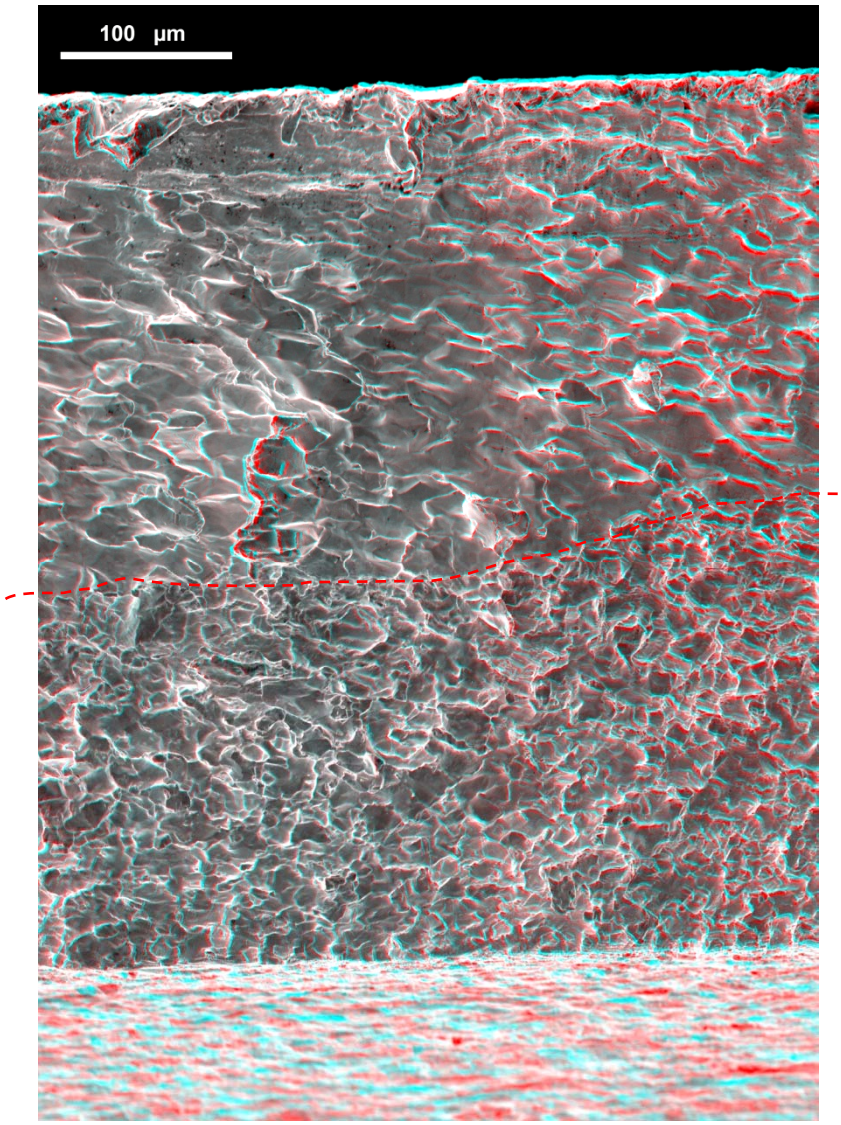

Figure 16.

The longitudinal fracture surface of a white gold tube opened by fire cracking is flat, even if observed tri-dimensionally. However, a morphological difference between the inner and the outer parts – respectively below and above the dashed line, is clearly visible.

When observed at higher magnification, the rupture turns out to be intergranular. The mean grain size changes abruptly along the tube section (figures 16). This is due to a highly un-homogeneous work hardening undergone by the material during metalworking, which leads to a different grain size during annealing.

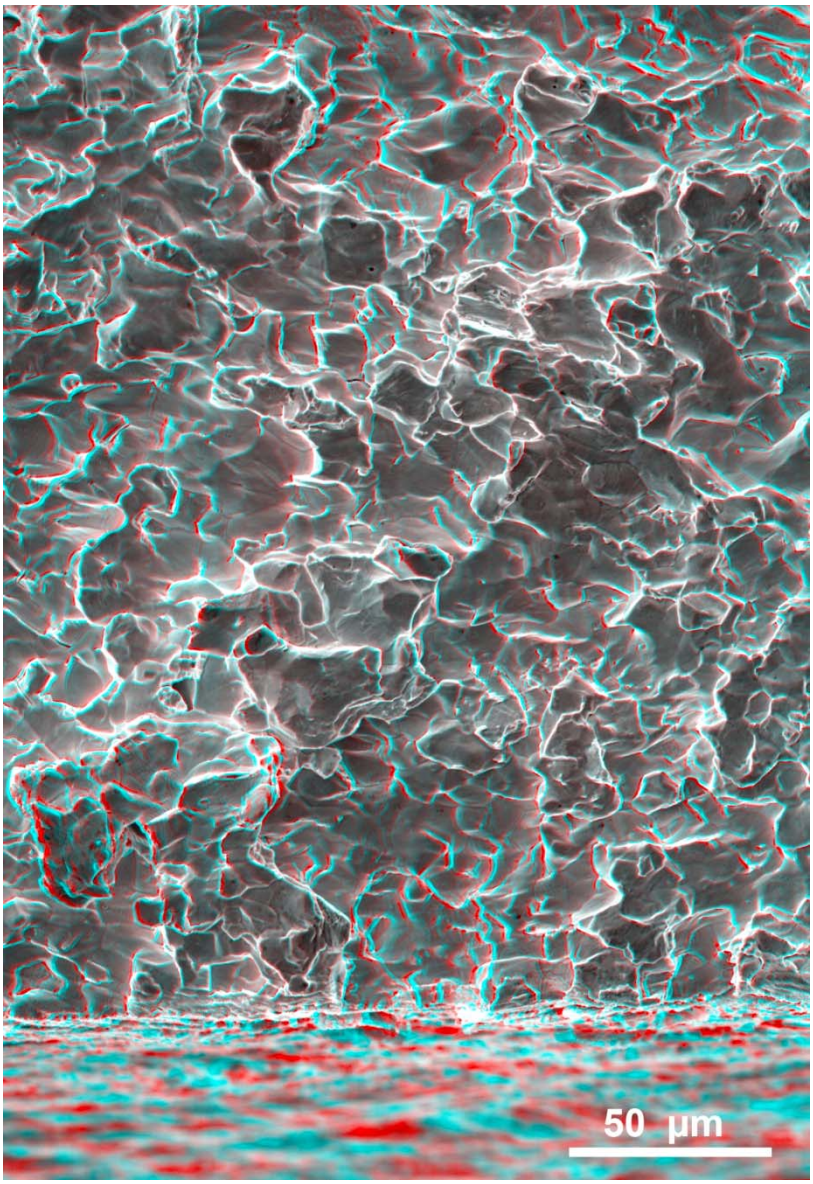

Figure 17.

Detail of the fracture surface of figure 16 below the dashed line, showing its characteristic intergranular morphology.

It is also interesting to observe the inner surface of the cracked tube (figure 18). In fact, many longitudinal wrinkles appear, as a result of a reduction of the inner diameter not compensated for by a mandrel. The wrinkles consist of deep grooves which may work as crack initiation sites during the annealing stages of the tube. The tri-dimensional observation allows for a better view of the depth of the wrinkles and their potential dangerousness as possible crack initiation sites.

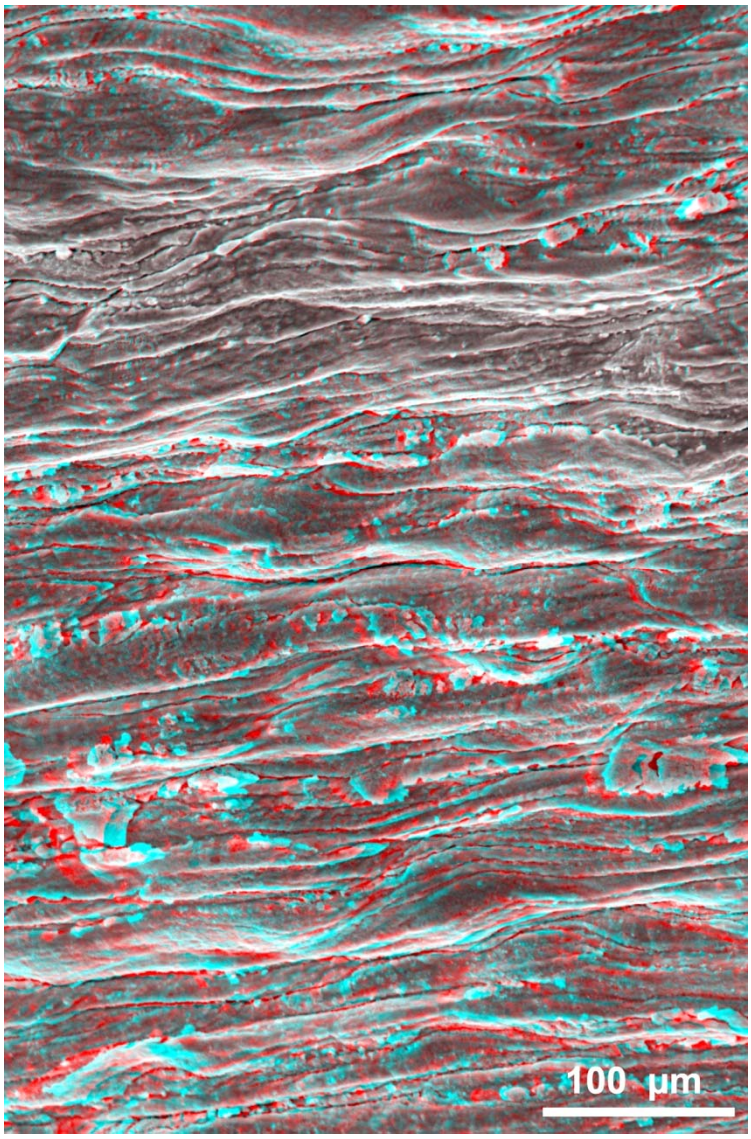

Figure 18.

The inner surface of the tube is completely wrinkled. The horizontal wrinkles are parallel to the longitudinal axis of the tube. The wrinkles are due to the forces applied during drawing, which reduces the inner diameter, unaided by a mandrel.

Surface finishing

The aspect of a surface depends on its microstructure. If particular aesthetic effects are to be obtained, the surface requires appropriate treatments and the final result depends on its microscopic tri-dimensional morphology. Specific geometrical effects are often observed, like in the following.

The three golden coins in figure 19 are examples. The 100-dollar coin on the left presents a background with a rather matt satin finish, showing up very clearly the figure in the middle, which has been given a mirror-like polish. The other two have a satin finish as well, but with different levels of dullness, lower in the 50-dollar coin.

Figure 19.

The three golden coins show different surface finishing.

Figure 20 shows the satin surface of the 100-dollar coin. It is made of scales placed on different planes one from the other. This makes the light diffuse in all directions, giving the surface the required dull aspect. At a higher magnification (figure 21), each scale reveals a rounded shape, further contributing to the dispersion of the incident light rays.

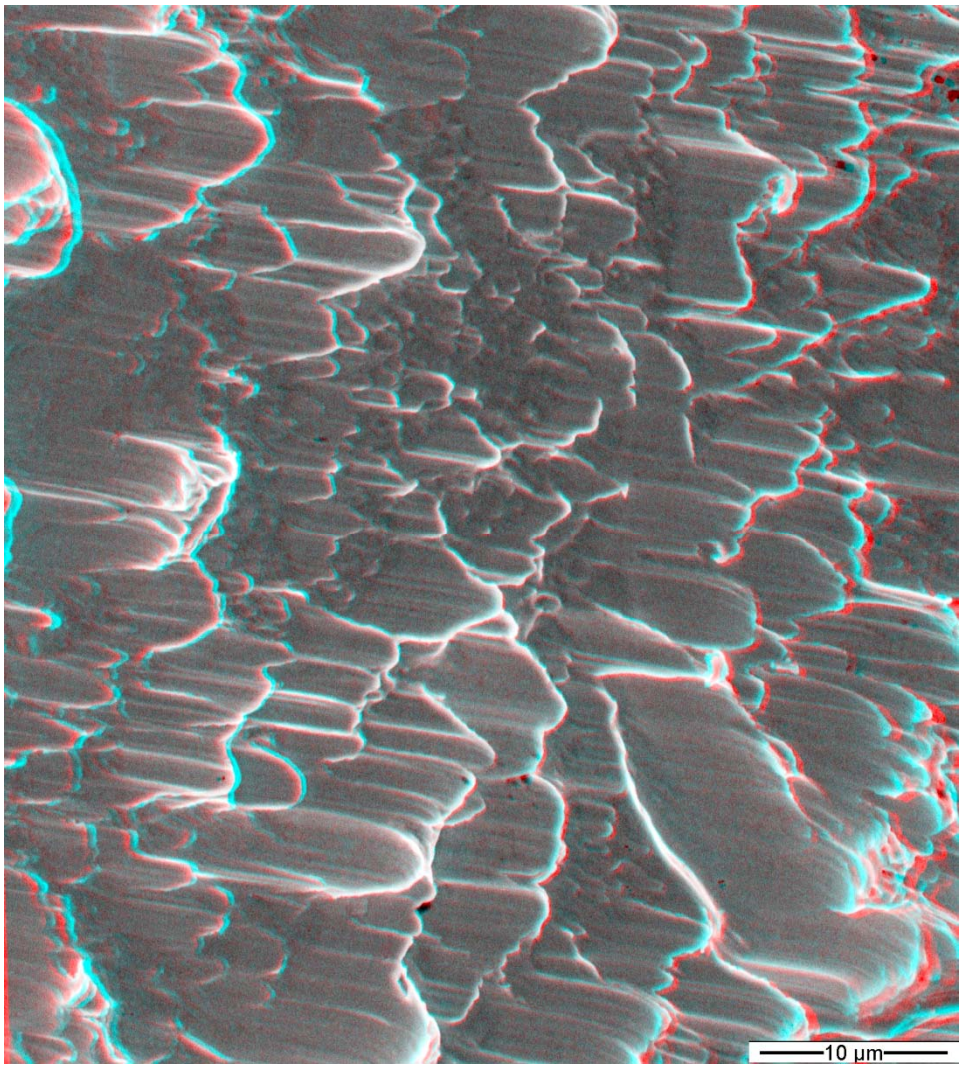

Figure 20.

The satin surface of the 100 dollar coins is made of scales, on different planes one from the other.

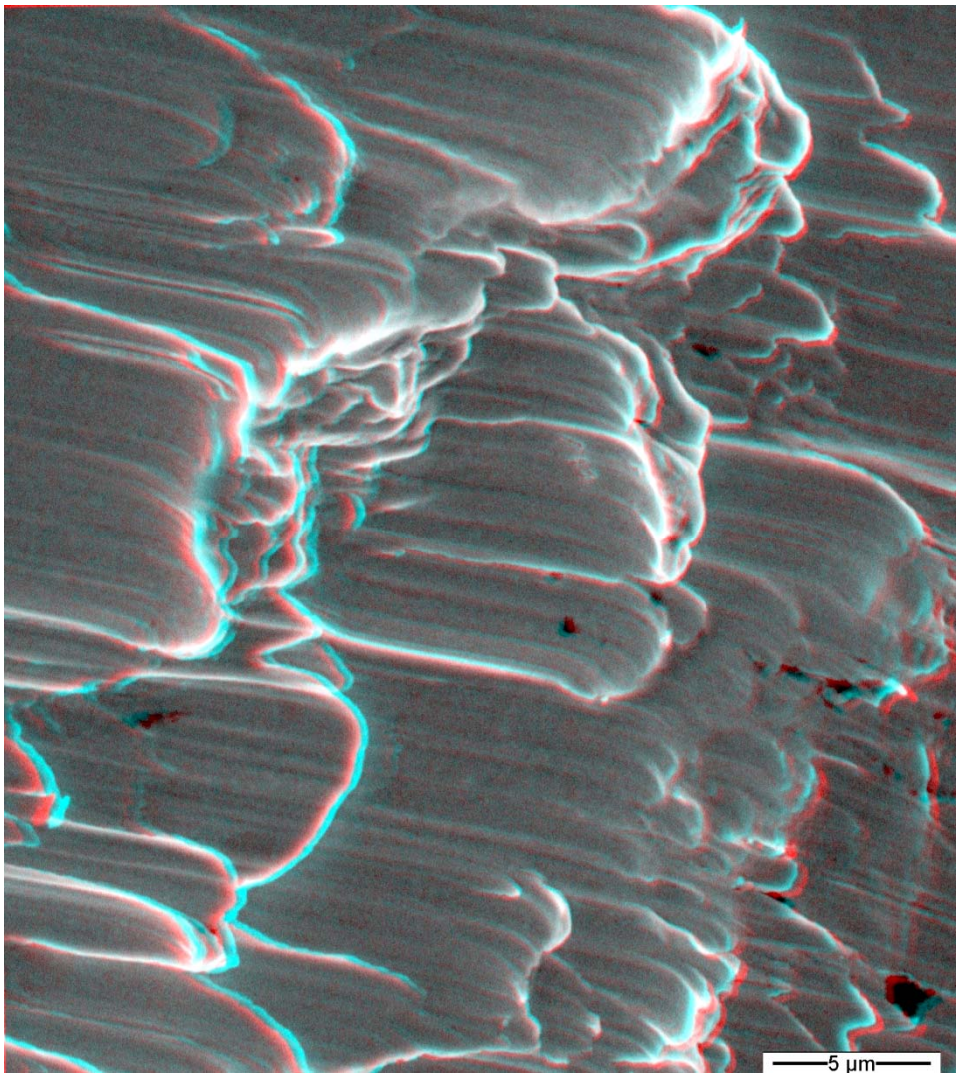

Figure 21.

When observed three-dimensionally, the surface in figure 20 shows round-shaped scales, which effectively contributes to giving the surface a dull aspect.

The 1000-Peso coin – in the middle in figure 19, shows a surface finishing similar to the previous one (figure 20), but with a lower definition of the scales, whose size is also higher (figure 22).
By comparing figures 22 and 20, whose magnification is the same, it is possible to understand why the surface of the 1000-Peso coin has a lower dullness and appears more brilliant.

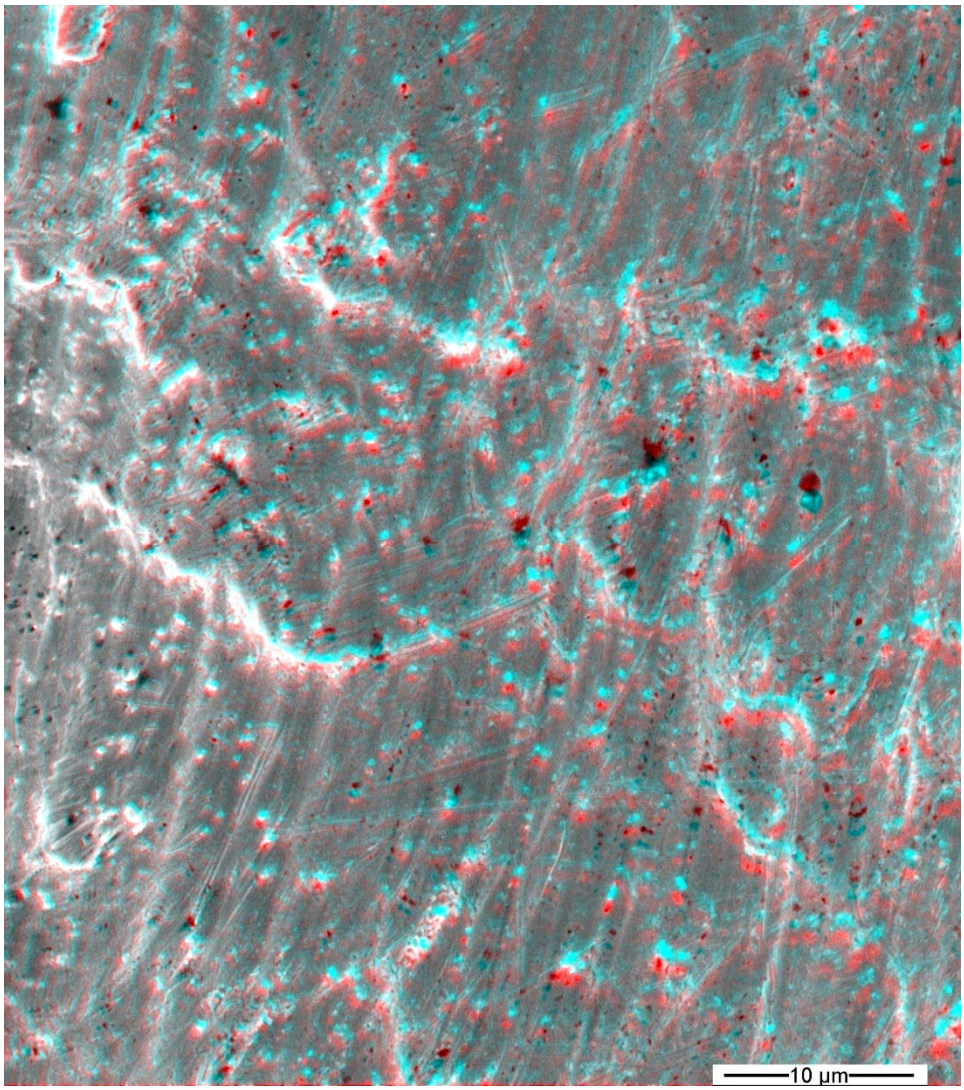

Figure 22.

Detail of the surface satin finishing of the 1000-Peso coin. If compared with figure 20, both figures having the same magnification, it can be understood why this microstructure gives rise to a brighter surface.

The 50-dollar coin shows an even smoother surface finishing, different from the previous two (figure 23). Figure 23 shows that flat and more reflecting zones are present on this surface, which does not happen in the other cases (see figures 20 and 22).

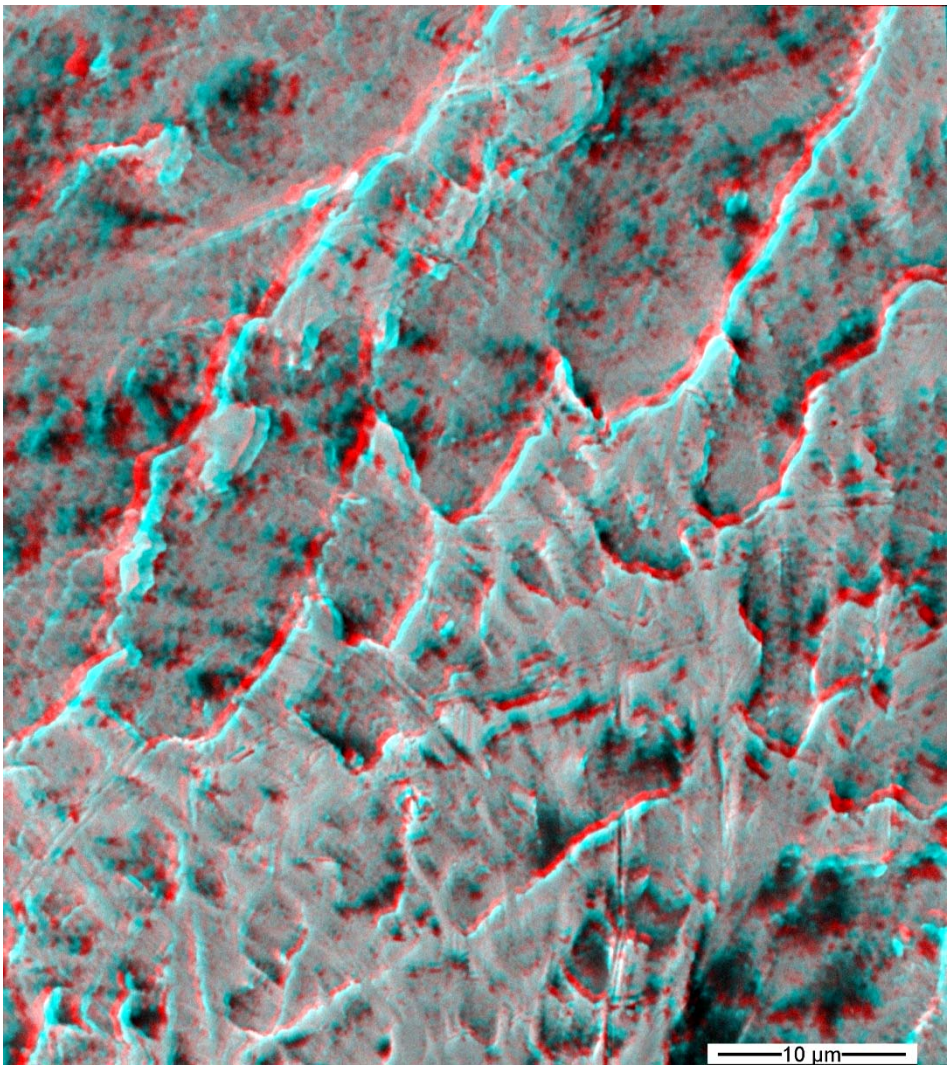

Figure 23.

This detail of the satin surface finishing of the 50-dollar coin can be compared with figures 20 and 22. Despite the occurrence of engravings in some regions, this surface is smoother as a whole, and more reflecting as a consequence. The lower part of this figure shows, for example, a smoother surface.

Sometimes, when a metal alloy is bent during metalworking, the so-called 'orange peel' phenomenon can occur, due to the fact that the crystal grains deform according to their orientation, which changes from grain to grain. As a consequence, a smooth surface becomes rough. Figure 24 shows an example of orange-peeling on an 18-carat red gold plate, bent by 90°. The higher the grain size, the more visible the orange-peel effect is.

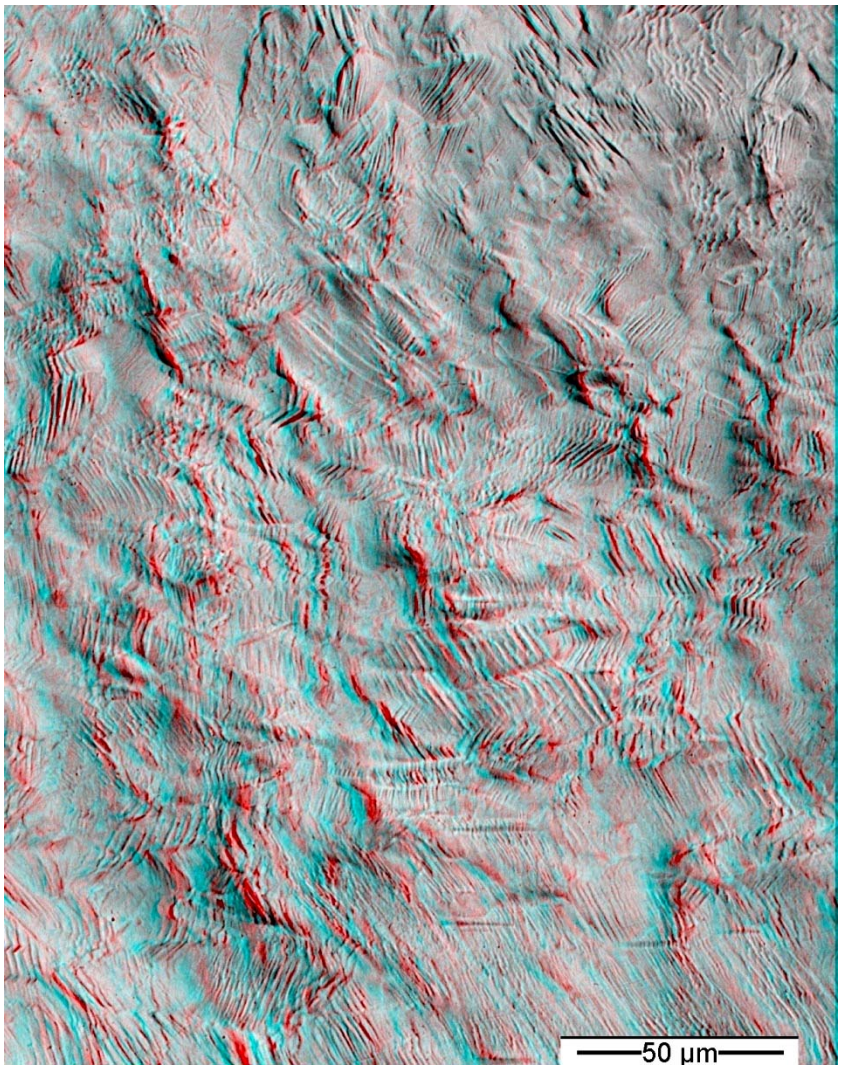

Figure 24.

The roughness visible on the surface of this 18-carat red gold plate appears after bending the material. Before that, the surface is flat and smooth. The small parallel steps discernible on the surface are due to crystal plane sliding along preferential directions, induced by the deformation of the alloy.

Another case in which small surface protuberances produce major aesthetical details is the so-called 'comet tails' case. This occurs when polishing a surface which presents hard inclusions firmly set in the material. The polishing process accumulates debris beside these hard particles and 'comet tails' develop. An example is given in figure 25. The SEM observation allows for a 3D view of these aesthetically highly dangerous defects (see Figures 26 and 27). It is possible to notice that it is not just a matter of material build-up, but also of excessive abrasion between inclusions next to one another.

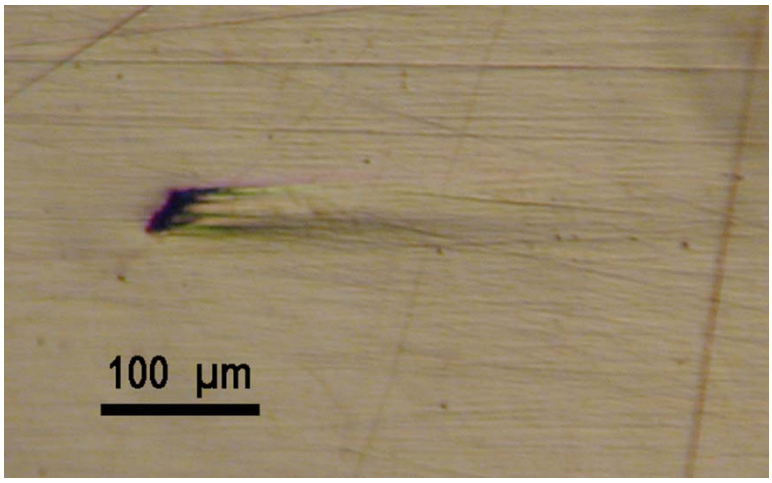

Figure 25.

Example of 'comet tail' as seen by optical microscopy.

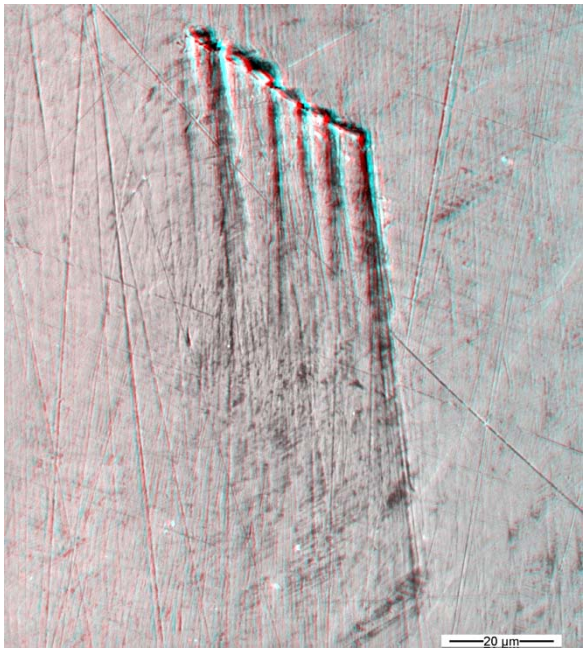

Figure 26.

The observation by SEM of the defect reported in figure 25 allows for the 3D view of the material debris which develops 'comet tails' below the hard inclusions.

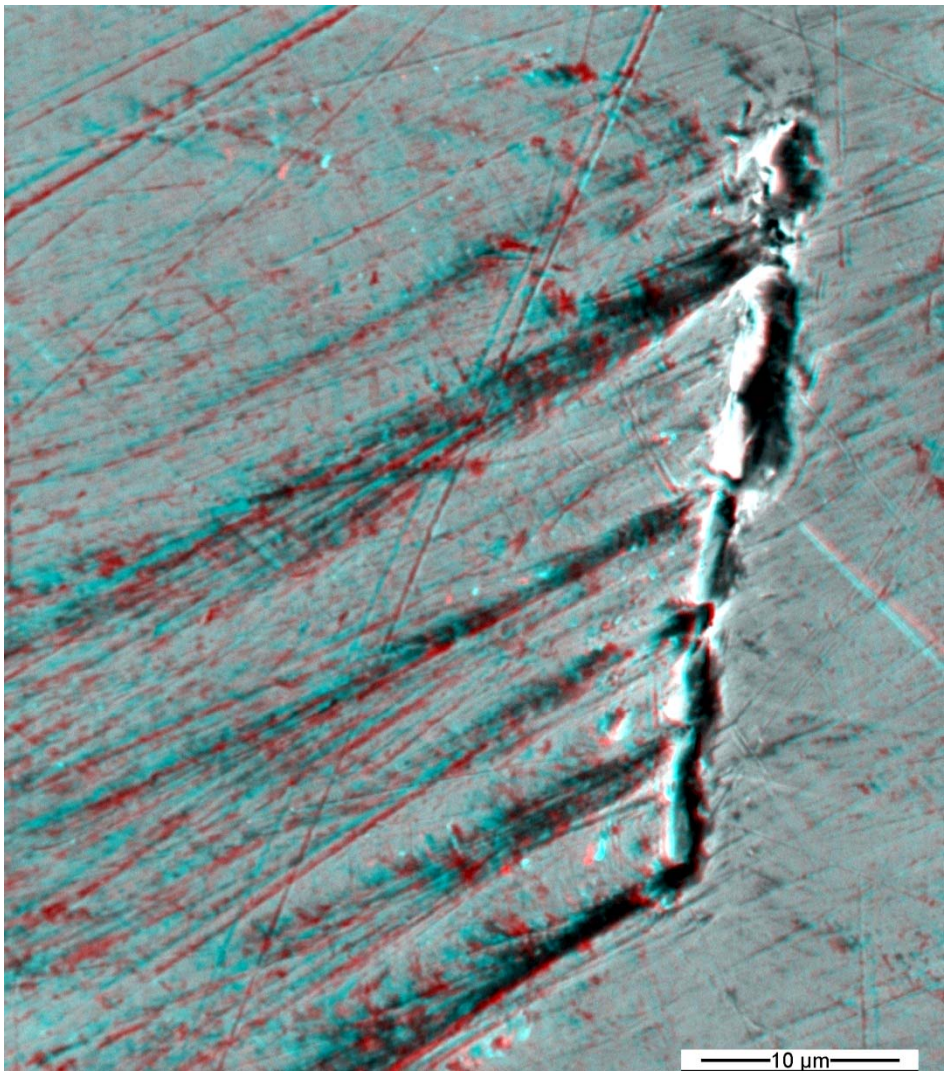

Figure 27.

Not only debris accumulation is detected by tri-dimensional observation, but also abrasion and grooves between these aligned defects appear. In this example the hard particles are made of aluminum oxide.

As cast surface.

When it comes to performing investment casting, the surface finishing obtained on the as cast material after the removal of the investment plays a major role. This finishing depends on many process parameters, but also on the kind of alloy which is being used. If the surface is smooth, it will allow for a more faithful reproduction of details and less finishing work. An optically irregular aspect of the surface is very often followed by complex microscopic morphologies, appreciable in tri-dimensions.
Figure 28 refers to the as cast surface of an object made of Sterling silver. To the naked eye the surface appears smooth.

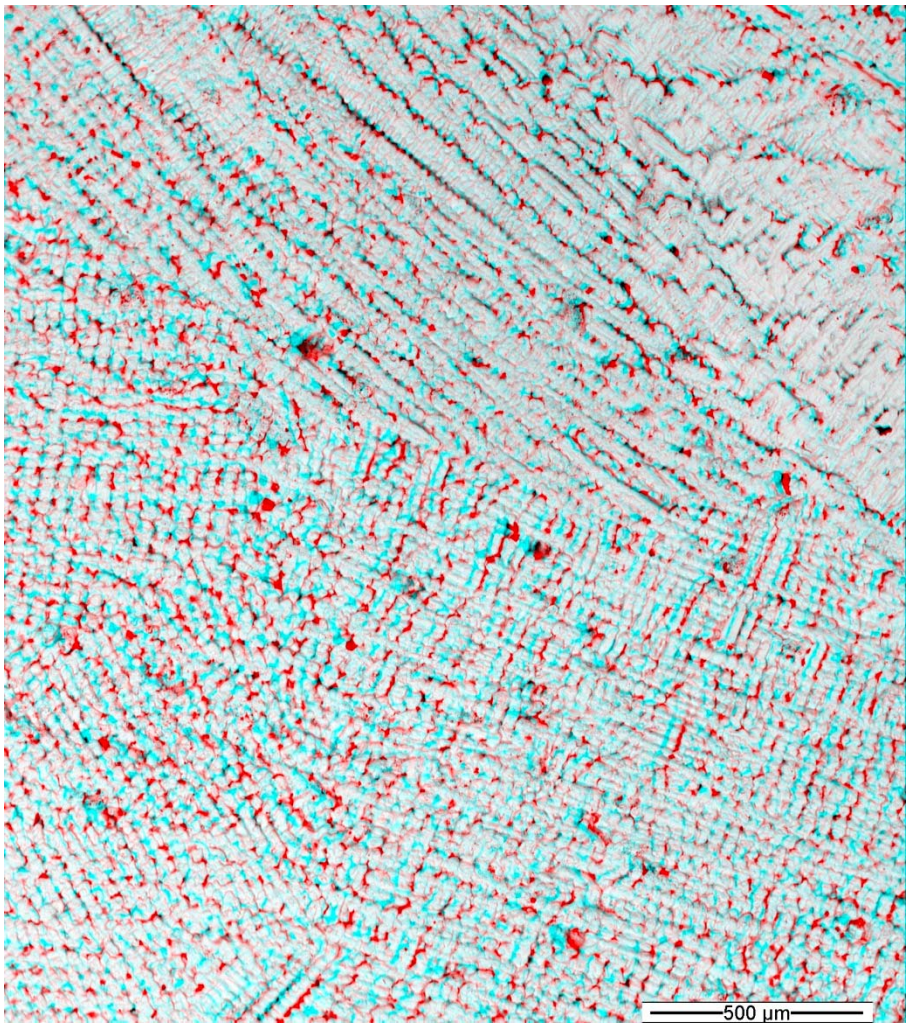

Figure 28.

As cast surface of a sample made of Sterling silver. To the naked eye the surface appears smooth. However, when observed by SEM - even at medium magnification, it shows an arrangement of closely spaced inter-dendritic pores.

However, when observed at a higher magnification, it shows an arrangement of closely spaced inter-dendritic pores (figure 29).

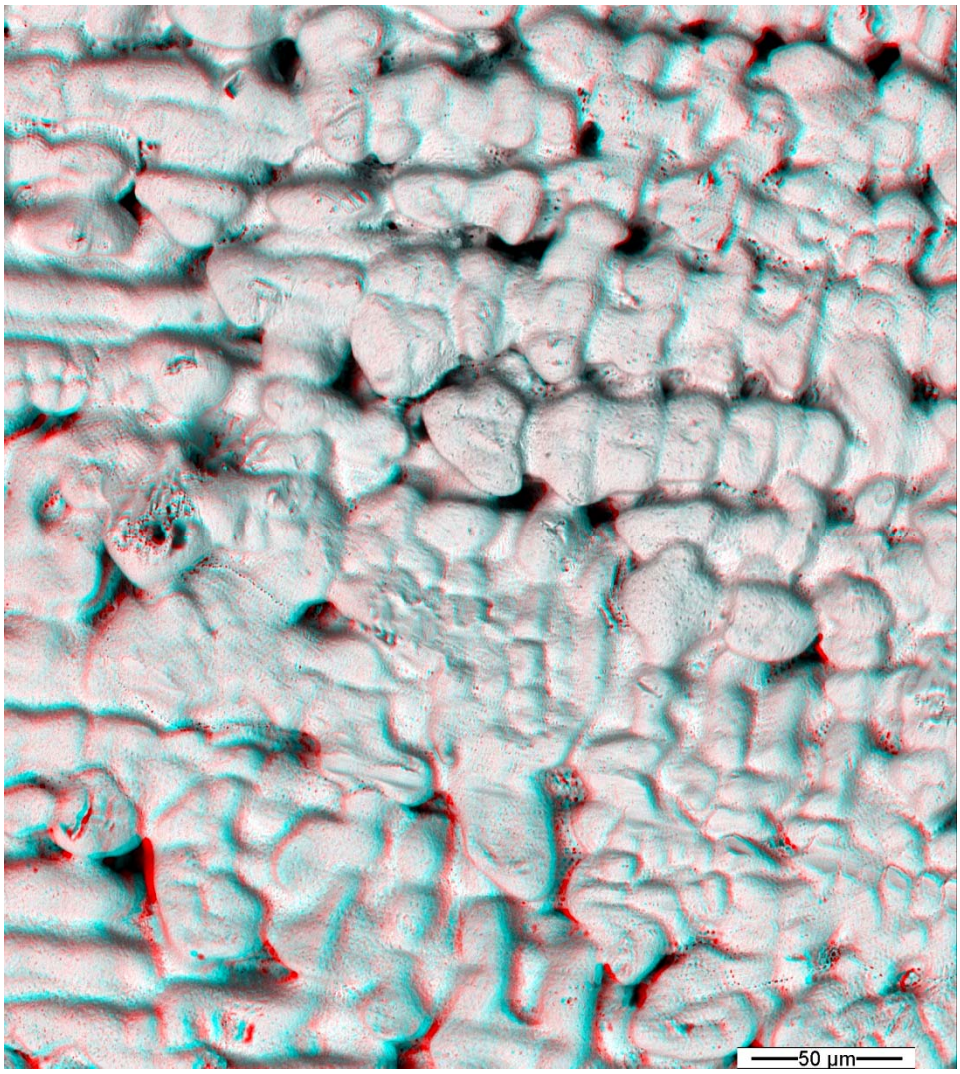

Figure 29.

Detail of figure 28 showing the presence of inter-dendritic pores and the roughness of the as cast surface.

Figure 28 refers to the as cast surface of a Pd 950 alloy. In this case another kind of roughness is revealed by tri-dimensional observation. In fact, round-shaped cavities are visible, probably due to gas release occurred at the contact between the investment and the alloy during the casting process.

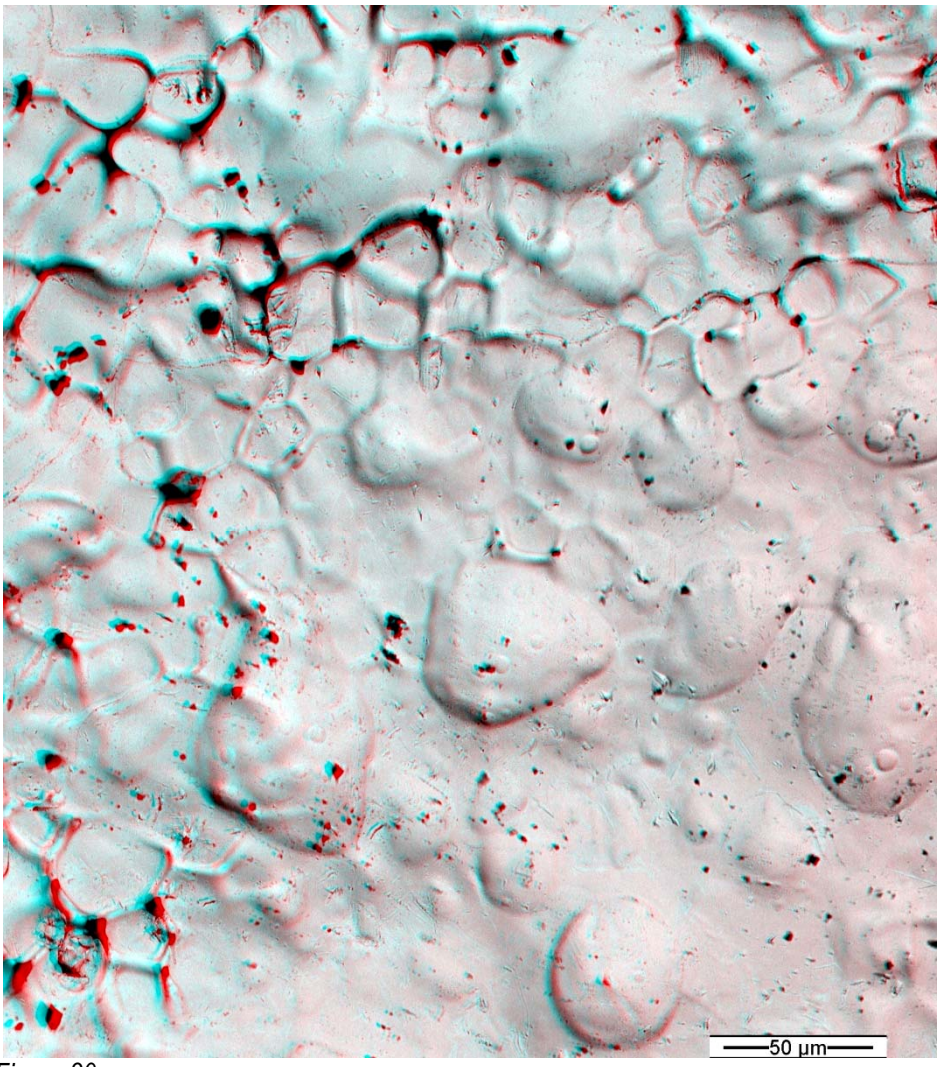

Figure 30.

As cast surface of a Pd 950 alloy. The surface is macroscopically smooth, but shows some small inter-dendritic pores and round-shaped cavities.

The surface of a 999 silver grain is an as cast surface as well. The expert eye is often able to recognize the contamination of silver, appearing as stains or halos on the grain surface. Figure 31 shows a silver grain contaminated by tin oxides. The tri-dimensional observation of its surface reveals why it is covered with opaque stains. The presence of tin oxide crystals increases the surface roughness, which appears more opaque as a consequence (figures 32 and 33)

Figure 31.

It is sometimes possible to recognize contamination in silver by observing its surface. Any stains or opaque regions are synonyms with contamination.

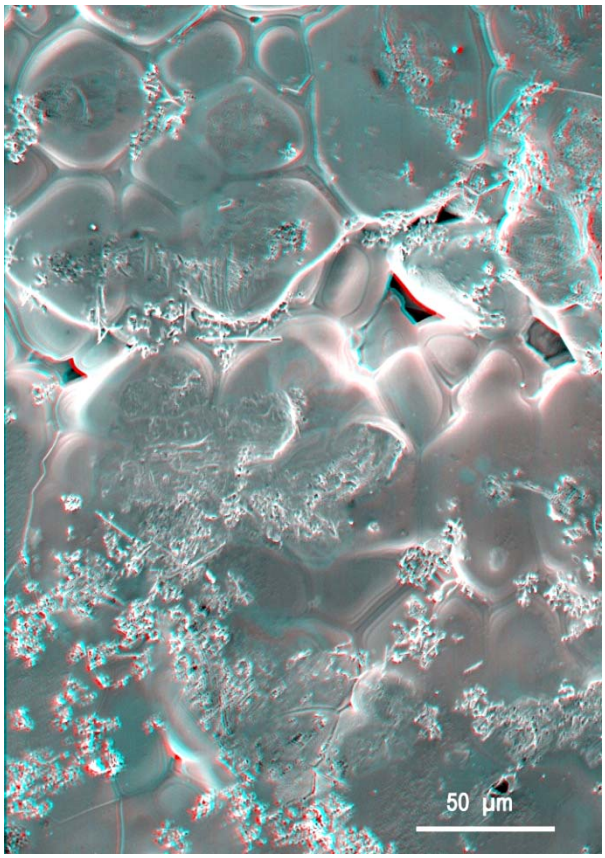

Figure 32.

Surface of the silver sample of figure 31. Its opaqueness is due to Tin oxides as well as pores.

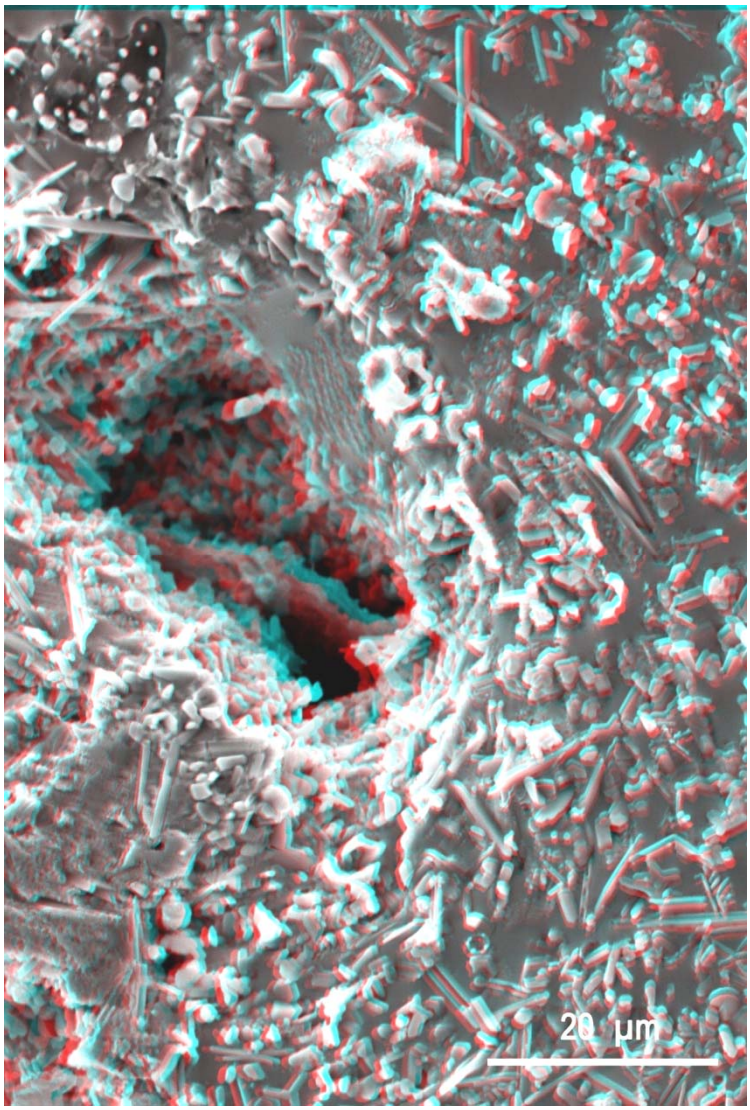

Figure 33.

Detail of figure 32. The tin oxides create a highly noticeable microscopic roughness and give the silver sample an opaque aspect.

Conclusions.

Scanning electron microscopy is a well established technique for microstructural analysis by means of the anaglyph technique. This technique - aided by the 3D observation, makes our brain able to understand more quickly and correctly the morphology of the analyzed surfaces. In fact, the reported examples have revealed some morphological features which would not have been easily recognizable by means of the bi-dimensional observation only. The anaglyph technique, well known for a long time, turns out to be a valuable tool to develop our knowledge of microstructures, which plays an unquestionable role in the goldsmith's field.

REFERENCES

1. *"Metallography and microstructures"* ASM Handbook, Volume 9, ASM International 2004 .
2. Porta Giovanni Battista: *De Refractione. Optices Parte. Libri Novem.* (Carlinum and Pacem, Naples, 1593).
3. N.J. Wade: *A natural history of vision.* (MIT Press, Cambridge MA, 1998).
4. *"Fractography"* ASM Handbook, Volume 12, ASM International 1987.
5. Vannoccio Biringuccio: *De La Pirotechnia (1540).*Kessinger Publishing, print on demand.
6. *"Failure Analysis and Prevention"* ASM Handbook, Volume 11, ASM International 2002.
7. Paolo Battaini, "Investment Casting Behavior of Palladium-Based Alloys", *The Santa Fe Symposium on Jewelry Manufacturing Technology 2008,* ed. Eddie Bell (Albuquerque: Met-Chem Research, 2008).
8. G. Normandeau , D. Ueno, "Fire Cracking in White Gold Jewelry Articles", *The Santa Fe Symposium on Jewelry Manufacturing Technology 2002,* ed. Eddie Bell (Albuquerque: Met-Chem Research, 2002).